IOCA 2021

MDPI

Article

Assessment of the seismic bearing capacity of strip footings over a void in heterogeneous soils: a Machine Learning-based approach

Mohammad Sadegh Es-haghi [1,*], Stefano Mariani [2]

[1] School of Civil Engineering, K. N. Toosi University of Technology, Tehran, Iran.
* Correspondence: ms_es.haghi@yahoo.com; stefano.mariani@polimi.it
[2] Department of Civil and Environmental Engineering, Politecnico di Milano, Piazza L. da Vinci 32, 20133 Milan, Italy.

Abstract: The estimation of the seismic bearing capacity of strip footing is of paramount importance in geotechnical engineering. In case of a shallow strip footing above voids in heterogeneous soil, the assessment of its said bearing capacity turns out to display a complex dependency on various parameters, linked to the geometry of the void and the properties of the soil. Recent research activities have highlighted that a methodology based on the combination of sensitivity analysis and machine learning can be extremely efficient in catching such a complex dependency. For the training of the ML technique, a database consisting of 38,000 Finite Element Limit Analysis (FELA) models has been adopted in this work. With the aim of estimating the mentioned seismic bearing capacity, five strategies have been investigated to select the training and test data. By considering the seismic bearing capacity as the single output parameter of the ML-based algorithm, and void depth and eccentricity, soil undrained shear strength and rate of change of its cohesion with the depth, and horizontal seismic acceleration as input parameters, the methodology has provided accurate results in mimicking the numerical, FELA-based reference solutions.

Keywords: Machine Learning; Shallow strip footing; Seismic bearing capacity; Finite element limit analysis; Heterogeneous soil.

Citation: Lastname, F.; Lastname, F.; Lastname, F. Title. *Algorithms* **2021**, *14*, x. https://doi.org/10.3390/xxxxx

Academic Editor: Firstname Lastname

Received: date
Accepted: date
Published: date

1. Introduction

The voids, especially in urban areas, may be located adjacent to or below shallow footings. The performance of strip footings can thus be significantly affected by the presence of the underground voids, which therefore require special attention in the design process. Several factors can quantify the effects of the voids on the footing bearing capacity, and they all have to be considered simultaneously to achieve an optimal design. To date, various studies have been conducted to investigate the bearing capacity of strip footings above voids, by using either theoretical or experimental methods, see e.g. [2-3, 4, 15-16, 28-29, 31, 37]. The Finite Element Limit Analysis (FELA) method has been recently adopted in [30], and design charts were obtained to estimate the ultimate bearing capacity of a strip footing over a rock mass with voids. In [36], the discontinuity layout optimization approach was used to determine the bearing capacity above square voids in cohesive-frictional soils, reporting typical failure patterns. The bearing capacity above multiple square voids was investigated in [21] for sandy soils and purely cohesive clays, also exploring the effect of load inclination. Lately, in [34] the impact of seismic loading on the bearing capacity for an undrained clay with voids was addressed.

In order to deal with complex problems, usually difficult to attack with a purely model-based approach, Machine Learning (ML) methodologies are currently finding a market, also in the civil engineering field, see e.g. [9-11, 22, 25, 27]. Regarding foundation engineering, Neural Networks have been employed so far to estimate the settlement and the load-carrying capacity of pile foundations [8, 20, 23] and of isolated shallow footings [1, 5, 12, 19, 26].

In the present study, a first attempt has been made to define a properly designed database dealing with the various factors affecting the bearing capacity of strip footings above a single unsupported void in either heterogeneous or homogenous soils, under seismic and quasi-static excitations. Results have been obtained as bounds on the load bearing capacity of the strip footing via the FELA method. First, a sensitivity analysis has been conducted to quantify the effects of these parameters on the ultimate footing bearing capacity. Next, to predict the seismic bearing capacity, the multiplayer perceptron (MLP) technique has been exploited.

2. Problem definition

In Figure 1, the (two-dimensional) geometry of the attacked problem is depicted. Assuming the strip footing and the tunnel to extend infinitely in the out-of-plane direction, plane strain conditions are adopted in the analysis. The strip footing is assumed rigid, featuring a rough contact with the heterogeneous soil. The following dimensionless variables are adopted to parametrize the problem:

- Horizontal seismic acceleration coefficient k_h, which is equal to the ratio between the horizontal earthquake-induced ground acceleration and the gravity acceleration.

- Ratio $\alpha = W/B$ between the void width W and the foundation width B.

- Ratio $\beta = H/B$ between the void height H and the foundation width B.

- Undrained shear soil strength $c_0/\gamma B$ at the ground level, where c_0 is the cohesion of the soil and γ the soil specific gravity.

- Rate of change kB/c_0 of the cohesion $c = c_0 + kz$ with the depth z. For a homogeneous soil k is null, whereas for heterogeneous soils k is positive.

- Internal friction angle φ of the soil in the drained state.

- Depth $D = Z/H$ of the void, where Z is the burial depth of the upper side (roof) of the void.

- Eccentricity $S = X/B$ of the void, where X is the horizontal distance of the center of the void from the centerline of the foundation.

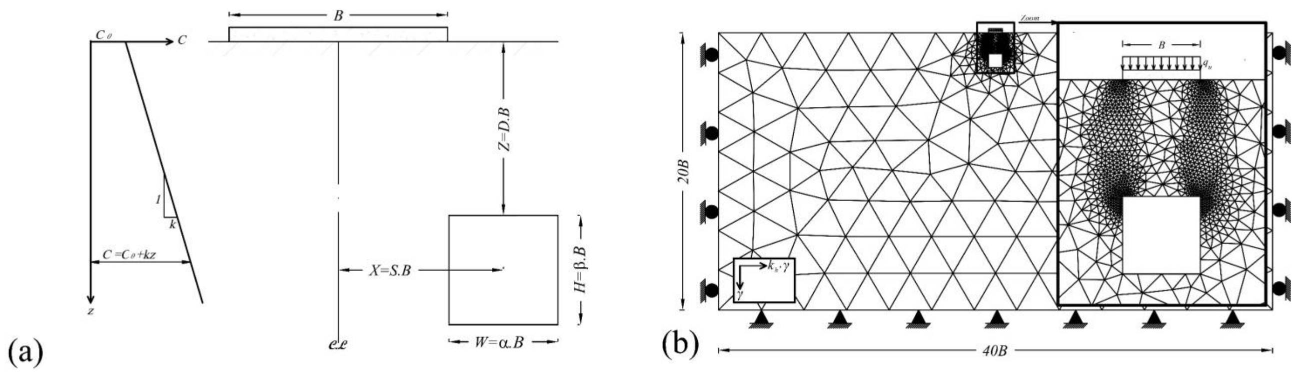

Fig 1. (a) Problem geometry, and (b) FELA mesh with a close-up depicting the adaptive refinement around the void.

Accounting for all the parameters listed above, the dimensionless undrained seismic ultimate bearing capacity Q of a strip footing placed above the void is given according to the law:

$$Q = \frac{q_u}{\gamma B} = f\left(\frac{c_0}{\gamma B}, \frac{kB}{c_0}, \varphi, S, D, \alpha, \beta, k_h\right) \quad (1)$$

FELA analyses have been carried out to determine Q by means of the Optum G2 software [17]. In the present analyses, a strip footing with a width $B = 1$ m is placed on a soil with a specific weight of 20 kN/m^3. To avoid perturbations to the solution induced by the boundaries of the domain of the soil, a geometry with a width of $40B$ and a depth of $20B$ has been considered. A uniformly distributed load has been applied on the footing, which has been assumed to grow until the formation of a collapse mechanism.

The pseudo-static method has been used to determine the seismic performance of the foundation over the cavity. The value of the horizontal acceleration coefficient k_h has been exploited, and once the upper and lower bounds on q_u at collapse have been computed; the mean value between these two bounds has been then assumed as representative for each model. An example of the adopted models is depicted in Figure 1, where the FELA adaptive mesh of the Optum G2 software, along with the adopted boundary conditions, are sketched.

To validate the modeling approach, a comparison with the studies of [6-7, 13-14, 18, 32-33, 35] has been made through the data gathered in Table 1. Such a comparison is provided in terms of the bearing capacity factor, at a varying value of the internal friction angle φ. The present results show a good agreement with those already published, and bound almost all of them.

Table 1. Bearing capacity of the foundation, in terms of the capacity factor.

φ (°)	N_γ									
	Present study		Yang et al.	Booker	Hansen	Chen	Michalowski	Kumar	Hjiaj et al.	Zhao and Yang
	LB	UB								
20	1.41	3.11	2.98	3.01	2.95	5.200	4.47	3.43	2.89	2.92
25	3.55	7.07	6.75	6.95	6.76	11.40	9.77	7.18	6.59	-
30	10.9	16.2	15.29	16.06	15.07	25.00	21.39	15.57	14.90	14.96
35	25.4	37.8	35.73	37.13	33.92	57.00	48.68	35.16	34.80	-
40	63.8	96.1	88.54	85.81	79.54	114.0	118.83	85.73	85.86	86.76

3. Parametric Study

A parametric analysis is discussed first. To evaluate the effect of the parameters listed in Section 2 on the seismic behavior of the system, a set of analyses has been run. The outcomes of this parametric analysis are next subdivided, to focus first on the parameters related to the soil behavior, and second on the parameters related to the geometry of the void.

3.1 Soil Parameters

Results in Figure 2 provide details regarding the variation of the dimensionless bearing capacity Q induced by the soil features, in case of different values of the horizontal seismic acceleration coefficient k_h. Figure 2(a) shows the outcome of the analysis for a broad range of values of the undrained shear strength. The graph shows that, for $c_0/\gamma B <$ 1, the model can be unstable: void collapse occurs without any loading and the value of Q is close to zero (though it cannot be computed due to the model instability). Regarding the effect of kB/c_0 on the seismic and static bearing capacity of the footing, Figure 2(b) also shows that the bearing capacity increases slightly under seismic conditions but then it becomes independent of kB/c_0. Results in Figure 2(c) finally show that, by increasing the angle of internal friction of the soil the bearing capacity of the strip footing increases too: for φ >30°, the bearing capacity keeps increasing sharply.

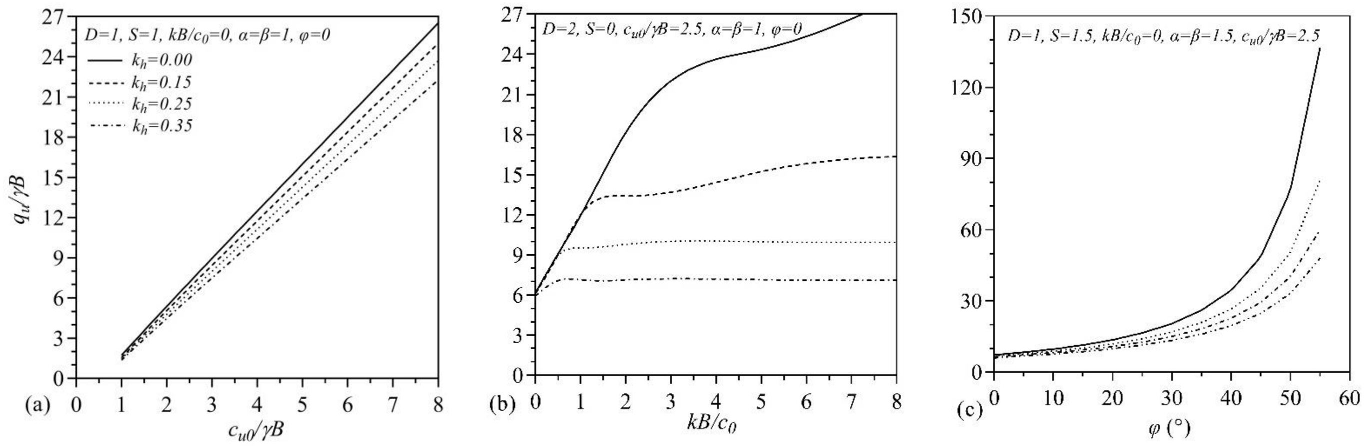

Fig. 2 Parametric analysis: effects on the bearing capacity Q, under different values of the seismic acceleration coefficient k_h, of the dimensionless soil parameters: (a) $c_0/\gamma B$; (b) kB/c_0; and (c) φ.

3.2 Void Parameters

Results of the parametric analysis are depicted in Figure 3, in terms of the evolution of the bearing capacity due to the void parameters related to shape and location. At constant seismic action measured through k_h, the capacity Q is shown to increase with the void depth D, till a saturation value that depends on k_h; similar conclusions can be provided by considering the horizontal distance S from the footing central line. It is also reported that the bearing capacity decreases if the ratio α linked to the void width increases, with instability for a value approaching $\alpha = 3$. For a void located below the midline of the footing, the ratio β related to the void height is shown to marginally reduce the bearing capacity, and then to attain a constant value.

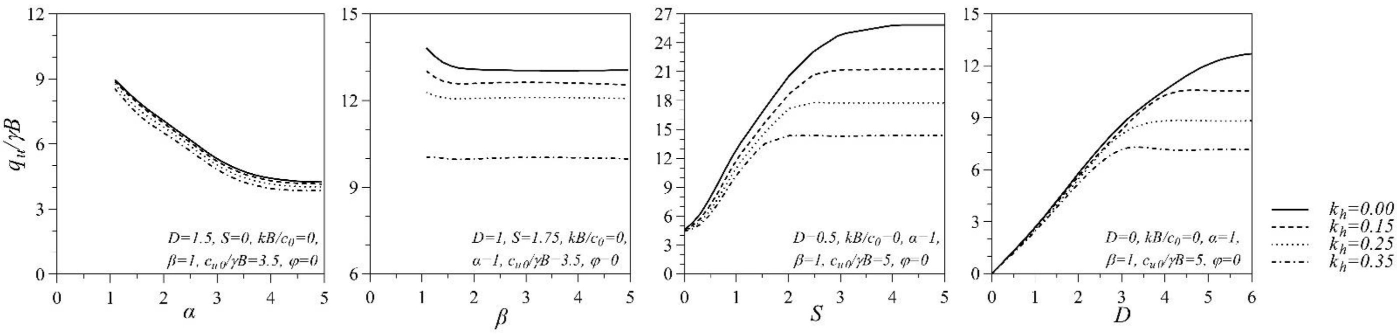

Fig. 3 Parametric analysis: effects on the bearing capacity Q, of the dimensionless void parameters: (a) α; (b) β; (c) S; and (d) D.

4. Machine learning techniques

To learn the seismic bearing capacity of shallow strip footing above the void, a nonlinear MLP algorithm has been adopted. The database to study is thus characterized by eight input parameters ($c_0/\gamma B$, kB/c_0, D, S, α, β, φ, and k_h) and only one output value ($Q = q_u/\gamma B$). A description of the adopted methodology is provided here, along with the impact of the relevant hyperparameters that control the learning process on the MLP performance.

MLP is a class of artificial neural networks (ANNs) and is an evolution of the perceptron neural network, see [24]. MLP is able to provide a nonlinear map $\mathbb{R}^k \longrightarrow \mathbb{R}^h$, in case of an input layer made of k neurons (input values) and an output layer made of h neurons (output values). It consists of an arbitrary number of hidden layers, with a variable number of neurons; the neurons are storage cells for scalar values, obtained by an activation function applied to the neuron values coming from the previous layer.

For our problem, a preliminary analysis has been performed to identify the optimal MLP architecture, in terms of number of neurons in the hidden layers to describe at best the correlation between input and output. In this regard, one-hidden-layer and two-hidden-layer ANNs have been investigated. Figure 4 provides a comparison among the behaviors of all the architectures allowed for, at the end of training. Results are reported in terms of the root mean square error (RMSE), given by:

$$\mathrm{RMSE} = \sqrt{\frac{1}{n}\sum_{i=1}^{n}(Q_{OG2\,i} - Q_{Model\,i})^2} \tag{2}$$

which represents the so-called loss function to be minimized during the training. In Eq. (2): n is the total number of data; for each analysis, $Q_{OG2\,i}$ is the load bearing capacity obtained with the Optum G2 software, while $Q_{Model\,i}$ is the value estimated by the MLP.

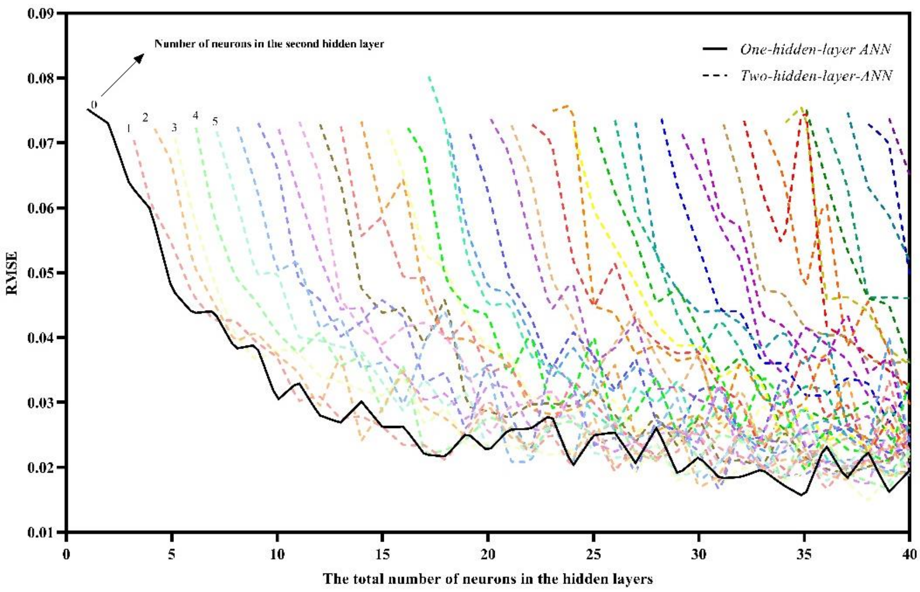

Fig. 4 Dependence of the RMSE at the end of training on the total number of neurons in the ANN, in case of either one or two hidden layers.

To assess the effects of the hyperparameters on the accuracy of the results, the plot shows the final value of RMSE as a function of the total number of neurons. The continuous line represents the solution obtained with one hidden-layer ANN; the dashed lines represent instead the solutions for the two hidden-layer ANNs, and for each of them a further label stands for the number of neurons in the second hidden layer. Each solution here has been computed as the average of ten repetitions of the training, to also assure robustness against stochastic effects.

What turns out from this additional parametric analysis is that the ANN featuring one hidden-layer only provides the best performances. For a number of neurons larger than 20 there is a marginal improvement in the accuracy of the results. Accordingly and to also minimize the computational costs of the entire procedure, the 8-20-1 ANN architecture has been adopted in the following.

5. Results and discussion

The performances of the selected MLP are now discussed. As metrics for them, the following statistical indices have been adopted to measure the discrepancy between the observed and the predicted values of the seismic load bearing capacity:

$$\mathrm{R}^2 = \left[\sum_{i=1}^{n}(Q_{OG2\,i} - \overline{Q_{OG2}})(Q_{Model\,i} - \overline{Q_{Model}}) \bigg/ \sqrt{\sum_{i=1}^{n}(Q_{OG2\,i} - \overline{Q_{OG2}})^2 \sum_{i=1}^{n}(Q_{Model\,i} - \overline{Q_{Model}})^2}\right]^2 \tag{3}$$

$$\mathrm{SI} = \mathrm{RMSE}/\overline{Q_{OG2}} \tag{4}$$

$$\mathrm{MAPE} = \frac{1}{n}\sum_{i=1}^{n} |Q_{OG2\,i} - Q_{Model\,i}|/Q_{OG2\,i} \quad (5)$$

$$\mathrm{BIAS} = \frac{1}{n}\sum_{i=1}^{n} (Q_{OG2\,i} - Q_{Model\,i}) \quad (6)$$

In the equations here above R^2, MAPE, SI, and BIAS are the coefficient of determination, the mean absolute percentage error, the scatter index, and the standard bias; besides them, the RMSE introduced above has been adopted too. The index $i = 1, \dots, n$ runs over the instances in the dataset; $\mathrm{Q}_{\mathrm{OG2\,i}}$ is the numerical value of the dimensionless load bearing capacity furnished by the Optum G2 software, while $Q_{Model\,i}$ is the corresponding value provided by the trained ML tool; the overbar means that the average value of the corresponding variables is allowed for.

Table 2 gathers the values of all the aforementioned statistical indices to assess the performance of the MLP. It can be seen that MLP is accurate in catching the structural response, as shown by the values of R^2, RMSE, SI, and BIAS. The same trend is depicted in the parity plots of Figure 5, where the estimations of the seismic bearing capacity of the shallow strip footing are compared with the ground-truth data. The output provided by MLP is well aligned with the perfect fit, represented by the bisector of the quadrant.

Table 2. Performance of MLP, in terms of the adopted statistical indices.

Algorithm	R^2	RMSE	MAPE	SI	BIAS
MLP	0.9955	0.0158	-0.0101	-0.0189	-0.0001

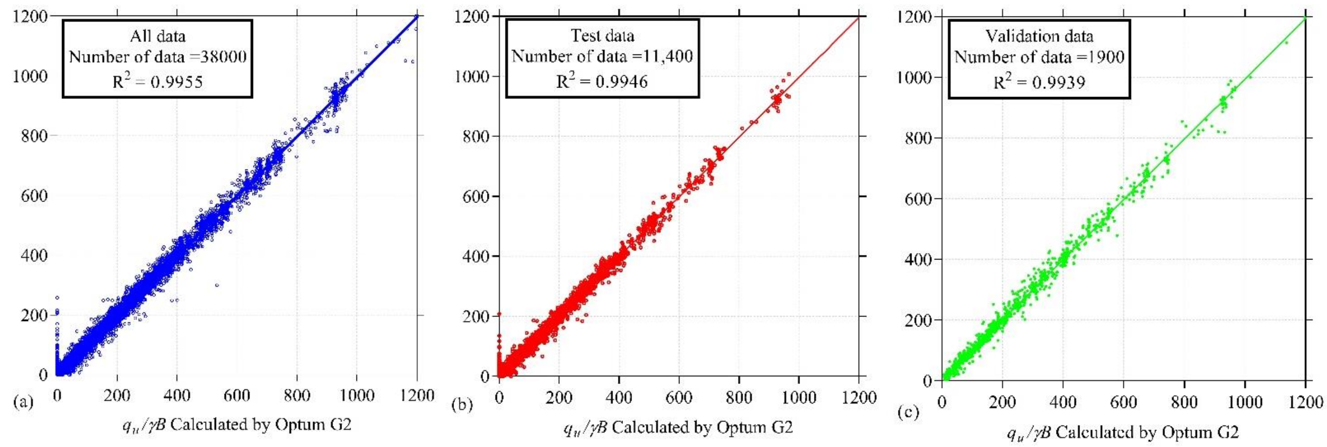

Fig. 5 Parity plots showing the MLP output against the corresponding ground-truth data linked to: (a) all the data; (b) test data; (c) validation data.

The accuracy of the results has been also investigated through a comparison between the FELA and the foreseen seismic bearing capacity of the shallow strip footing, see Figure 6. For this comparative visualization only, 1% of the instances in the dataset has been randomly selected to provide a clearer vision of the quality of data fitting. The seismic bearing capacity computed by MLP matches quite well the FELA counterpart, with a bounded scattering in accordance with the results of Figure 5.

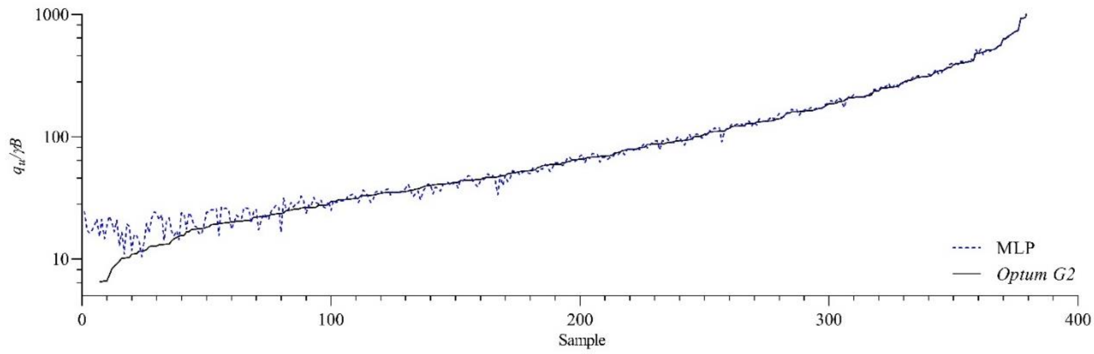

Fig. 6 Comparison between the FELA results and those forecasted by the MLP.

6. Conclusion

In this study, the seismic bearing capacity of a strip footing placed over an unsupported void has been studied by means of a data-driven approach. Dimensionless factors describing the horizontal seismic acceleration, the soil strength and heterogeneity, the internal friction angle of the soil, the shape, size, depth, and eccentricity of the void have been all accounted for. A MLP has been adopted to estimate the mentioned bearing capacity. The hyperparameters affecting the performance of the MLP have been optimized in order to maximize the accuracy of the solution. The results obtained by training the MLP have shown a good fitting of the seismic bearing capacity computed with time-demanding numerical FELA simulations, handled in the present study as ground-truth data.

Only rectangular voids have been considered here. Having established the accuracy of the proposed methodology, additional data will be handled in future activities to allow for voids with different geometries, in order to generalize the procedure and make it void shape-independent.

Author Contributions: Conceptualization, M.S.E. and S.M.; methodology, M.S.E. and S.M.; software, M.S.E.; validation, M.S.E.; formal analysis, M.S.E; investigation, M.S.E. and S.M.; resources, M.S.E. and S.M.; data curation, M.S.E.; writing—original draft preparation, M.S.E. and S.M.; writing—review and editing, M.S.E. and S.M.; visualization, M.S.E.; supervision, S.M.; project administration, S.M.; All authors have read and agreed to the published version of the manuscript.

Funding: This research received no external funding.

Data Availability Statement: Data, models, and codes that support the findings of this study are available from the corresponding author upon request.

Conflicts of Interest: The authors declare no conflict of interest.

References

1. Acharyya R, Dey A. Assessment of failure mechanism of a strip footing on horizontal ground considering flow rules. Innovative Infrastructure Solutions. 2018 Dec;3(1):1-6.
2. Al-Tabbaa A, Russell L, O'Reilly M. Model tests of footings above shallow cavities. Ground Engineering. 1989 Oct;22(7).
3. Badie A, Wang MC. Stability of spread footing above void in clay. Journal of Geotechnical Engineering. 1984 Nov;110(11):1591-605.
4. Baus RL, Wang MC. Bearing capacity of strip footing above void. Journal of Geotechnical Engineering. 1983 Jan;109(1):1-4.
5. Behera RN, Patra CR, Sivakugan N, Das BM. Prediction of ultimate bearing capacity of eccentrically inclined loaded strip footing by ANN: Part II. International Journal of Geotechnical Engineering. 2013 Apr 1;7(2):165-72.
6. Booker JR. Application of theories of plasticity to cohesive frictional soils.
7. Chen W-F. Limit Analysis and Soil Plasticity. Elsevier Science; 1975.
8. Das SK, Basudhar PK. Undrained lateral load capacity of piles in clay using artificial neural network. Computers and Geotechnics. 2006 Dec 1;33(8):454-9.
9. Das SK, Samui P, Sabat AK. Application of artificial intelligence to maximum dry density and unconfined compressive strength of cement stabilized soil. Geotechnical and Geological Engineering. 2011 May;29(3):329-42.

10. Erzin Y, Gumaste SD, Gupta AK, Singh DN. Artificial neural network (ANN) models for determining hydraulic conductivity of compacted fine-grained soils. Canadian Geotechnical Journal. 2009 Aug;46(8):955-68.
11. Es-Haghi MS, Shishegaran A, Rabczuk T. Evaluation of a novel Asymmetric Genetic Algorithm to optimize the structural design of 3D regular and irregular steel frames. Frontiers of Structural and Civil Engineering. 2020 Aug;14(5):1110-30.
12. Giasi CI, Cherubini C, Paccapelo F. Evaluation of compression index of remoulded clays by means of Atterberg limits. Bulletin of Engineering Geology and the Environment. 2003 Nov;62(4):333-40.
13. Hansen, JB. "A Revised and Extended Formula for Bearing Capacity." Dan Geotech Inst, Copenhagen, Bull. 1970; 28: 5–11.
14. Hjiaj, M., Lyamin, A. V., & Sloan, S. W. Numerical limit analysis solutions for the bearing capacity factor Nγ. International Journal of Solids and Structures. 2005, 42(5-6), 1681-1704.
15. Kiyosumi M, Kusakabe O, Ohuchi M. Model tests and analyses of bearing capacity of strip footing on stiff ground with voids. Journal of geotechnical and geoenvironmental engineering. 2011 Apr 1;137(4):363-75.
16. Kiyosumi M, Kusakabe O, Ohuchi M, Le Peng F. Yielding pressure of spread footing above multiple voids. Journal of geotechnical and geoenvironmental engineering. 2007 Dec;133(12):1522-31.
17. Krabbenhoft K, Lyamin A, Krabbenhoft J. Optum computational engineering (OptumG2). Computer software]. Retrieved from https://www. optumce. com. 2015.
18. Kumar J. N γ for rough strip footing using the method of characteristics. Canadian Geotechnical Journal. 2003 Jun 1;40(3):669-74.
19. Kuo YL, Jaksa MB, Lyamin AV, Kaggwa WS. ANN-based model for predicting the bearing capacity of strip footing on multi-layered cohesive soil. Computers and Geotechnics. 2009 Apr 1;36(3):503-16.
20. Lee IM, Lee JH. Prediction of pile bearing capacity using artificial neural networks. Computers and geotechnics. 1996 Jan 1;18(3):189-200.
21. Lee JK, Kim J. Stability charts for sustainable infrastructure: Collapse loads of footings on sandy soil with voids. Sustainability. 2019 Jan;11(14):3966.
22. Mishra AK, Kumar B, Dutta J. Prediction of Hydraulic Conductivity of Soil Bentonite Mixture Using Hybrid-ANN Approach. Journal of Environmental Informatics. 2016 Jun 1;27(2).
23. Momeni E, Nazir R, Armaghani DJ, Maizir H. Prediction of pile bearing capacity using a hybrid genetic algorithm-based ANN. Measurement. 2014 Nov 1;57:122-31.
24. Noriega, L. Multilayer perceptron tutorial. School of Computing. Staffordshire University. 2005
25. Safari MJ, Ebtehaj I, Bonakdari H, Es-haghi MS. Sediment transport modeling in rigid boundary open channels using generalize structure of group method of data handling. Journal of Hydrology. 2019 Oct 1;577:123951.
26. Shahin MA, Maier HR, Jaksa MB. Predicting settlement of shallow foundations using neural networks. Journal of Geotechnical and Geoenvironmental Engineering. 2002 Sep;128(9):785-93.
27. Shishegaran A, Varaee H, Rabczuk T, Shishegaran G. High correlated variables creator machine: Prediction of the compressive strength of concrete. Computers & Structures. 2021 Apr 15;247:106479.
28. Wang MC, Badie A. Effect of underground void on foundation stability. Journal of Geotechnical Engineering. 1985 Aug;111(8):1008-19.
29. Wang MC, Hsieh CW. Collapse load of strip footing above circular void. Journal of geotechnical engineering. 1987 May;113(5):511-5.
30. Xiao Y, Zhao M, Zhao H, Zhang R. Finite element limit analysis of the bearing capacity of strip footing on a rock mass with voids. International Journal of Geomechanics. 2018 Sep 1;18(9):04018108.
31. Yamamoto K, Lyamin AV, Wilson DW, Sloan SW, Abbo AJ. Stability of dual circular tunnels in cohesive-frictional soil subjected to surcharge loading. Computers and Geotechnics. 2013 May 1;50:41-54.
32. Yang F, Zheng XC, Zhao LH, Tan YG. Ultimate bearing capacity of a strip footing placed on sand with a rigid basement. Computers and Geotechnics. 2016 Jul 1;77:115-9.
33. Yun G, Bransby MF. The undrained vertical bearing capacity of skirted foundations. Soils and foundations. 2007 Jun 1;47(3):493-505.
34. Zhang R, Feng M, Xiao Y, Liang G. Seismic Bearing Capacity for Strip Footings on Undrained Clay with Voids. Journal of Earthquake Engineering. 2020 Nov 27:1-4.
35. Zhao LH, Yang F. Construction of improved rigid blocks failure mechanism for ultimate bearing capacity calculation based on slip-line field theory. Journal of Central South University. 2013 Apr 1;20(4):1047-57.
36. Zhou H, Zheng G, He X, Xu X, Zhang T, Yang X. Bearing capacity of strip footings on c–φ soils with square voids. Acta Geotechnica. 2018 Jun;13(3):747-55..
37. Es-haghi MS, Abbaspour M, Rabczuk T. Factors and Failure Patterns Analysis for Undrained Seismic Bearing Capacity of Strip Footing Above Void. International Journal of Geomechanics. 2021 Oct 1;21(10):04021188.